
Authors

Andrés Holz, Juan Paritsis, Ignacio A Mundo, Thomas T Veblen, Thomas Kitzberger, Grant J Williamson, Ezequiel Aráoz, Carlos Bustos-Schindler, Mauro E González, H Ricardo Grau, and Juan M Quezada

Southern Annular Mode drives multi-century wildfire activity in southern South America

Andrés Holz¹, Juan Paritsis², Ignacio Mundo³, Thomas Veblen⁴, Thomas Kitzberger⁵, Grant Williamson⁶, Ezequiel Aráoz⁷, Carlos Bustos-Schindler⁸, Mauro González⁹, H. Grau¹⁰, Juan Quezada¹¹

¹Portland State University, ²Universidad Nacional del Comahue, ³CONICET, CCT-Mendoza, ⁴University of Colorado, Boulder, ⁵Laboratorio Ecotono, INIBIOMA-CONICET, Universidad Nacional del Comahue, Bariloche, Argentina, ⁶University of Tasmania, ⁷Universidad Nacional de Tucumán-CONICET, ⁸Instituto de Silvicultura, ⁹Universidad Austral de Chile, ¹⁰Universidad Nacional de Tucumán, ¹¹Universidad Nacional de Misiones, Eldorado

Submitted to Proceedings of the National Academy of Sciences of the United States of America

The Southern Annular Mode (SAM) is the main driver of climate variability at mid-to-high latitudes in the Southern Hemisphere affecting wildfire activity which in turn pollutes the air and contributes to human health problems and mortality, and potentially has a strong feedback to the climate system through emissions and land cover change. Here we develop the largest southern hemisphere network of annually-resolved tree-ring fire histories (see SI Appendix, Table S1.) consisting of 1767 fire-scarred trees from 97 sites (from 22 to 54°S latitude) to quantify the coupling of SAM and regional wildfire variability using recently created multi-century proxy indices of SAM for the period 1531 to 2010 AD. We show that at interannual time scales as well as at multidecadal time scales across the 37 to 54°S latitudinal gradient elevated wildfire activity is synchronous with positive phases of the SAM over the period from 1665 to 1995 AD. Positive phases of the SAM are primarily associated with warm conditions in these biomass-rich forests in which widespread fire activity depends on fuel desiccation. Climate modeling studies indicate that greenhouse gases will force SAM into its positive phase even if stratospheric ozone returns to normal levels, so that climate conditions conducive to widespread fire activity in southern South America (SSA) will continue throughout the 21st century.

fire scars | climate modes | AAO | synchrony

Introduction

Fire is a key ecological process in southern South America (SSA) and affects ecosystem dynamics and services (1), and smoke-related human health (2). Fire activity in SSA is primarily driven by variation in fuel amount and condition, ignition patterns, and climate variability (3, 4). In SSA, wildfire activity is related to large-scale climate modes (e.g. ENSO) as evidenced in landscape-scale tree-ring fire histories typically spanning about two degrees of latitude (5-7) and in modern documentary fire records across biomes from semi-arid to rainforest ecosystems (3). Understanding fire-climate relationships can clarify the relative importance of humans in either increasing or decreasing wildfire activity, and allow land managers to better anticipate future fire activity under climate change (3). To date however, there have been no broad-scale syntheses of long-term (i.e. multi-century) fire activity and climate-fire dynamics for anywhere in the Southern Hemisphere.

Since the 1950s at mid-high latitudes in the Southern Hemisphere there has been rise in temperature during the growing season (Fig. 1a), a phenomenon largely attributed to an intensification and poleward shift of the Southern Hemisphere Westerlies (8-10) associated variability of the Southern Annular Mode (SAM) (11), Fig. 1b). During this period the SAM has experienced an upward (positive) trend during spring and summer (Fig. 1c) attributed to stratospheric ozone depletion and increases in greenhouse gases (12) which is unprecedented over the last 1,000 years (13). As the leading pattern of tropospheric circulation variability south of 20°S, the SAM is essentially a zonally symmetric or annular structure, with synchronous, see-saw-like anomalies of opposite signs in Antarctica and the midlatitudes (ca. 40-50°S)

(8). During the SAM's positive phase decreased (increased) surface pressure and geopotential heights are observed over Antarctica (midlatitudes) and the southern westerly winds strengthen and shift poleward, while opposite conditions prevail during its negative phase (8, 14). For SSA this SAM-mediated increase in surface pressure and geopotential heights act like a blocking pressure system that since the 1950s has been associated with a) warmer conditions due to a combination of enhanced horizontal advection, subsidence and solar radiation (15) (particularly south of 40°S and during summer) (14), and b) with dry conditions due to reduced frontal and orographic precipitation (16) and weakening of the moisture convergence (17) (particularly at 40°S and during spring) (14).

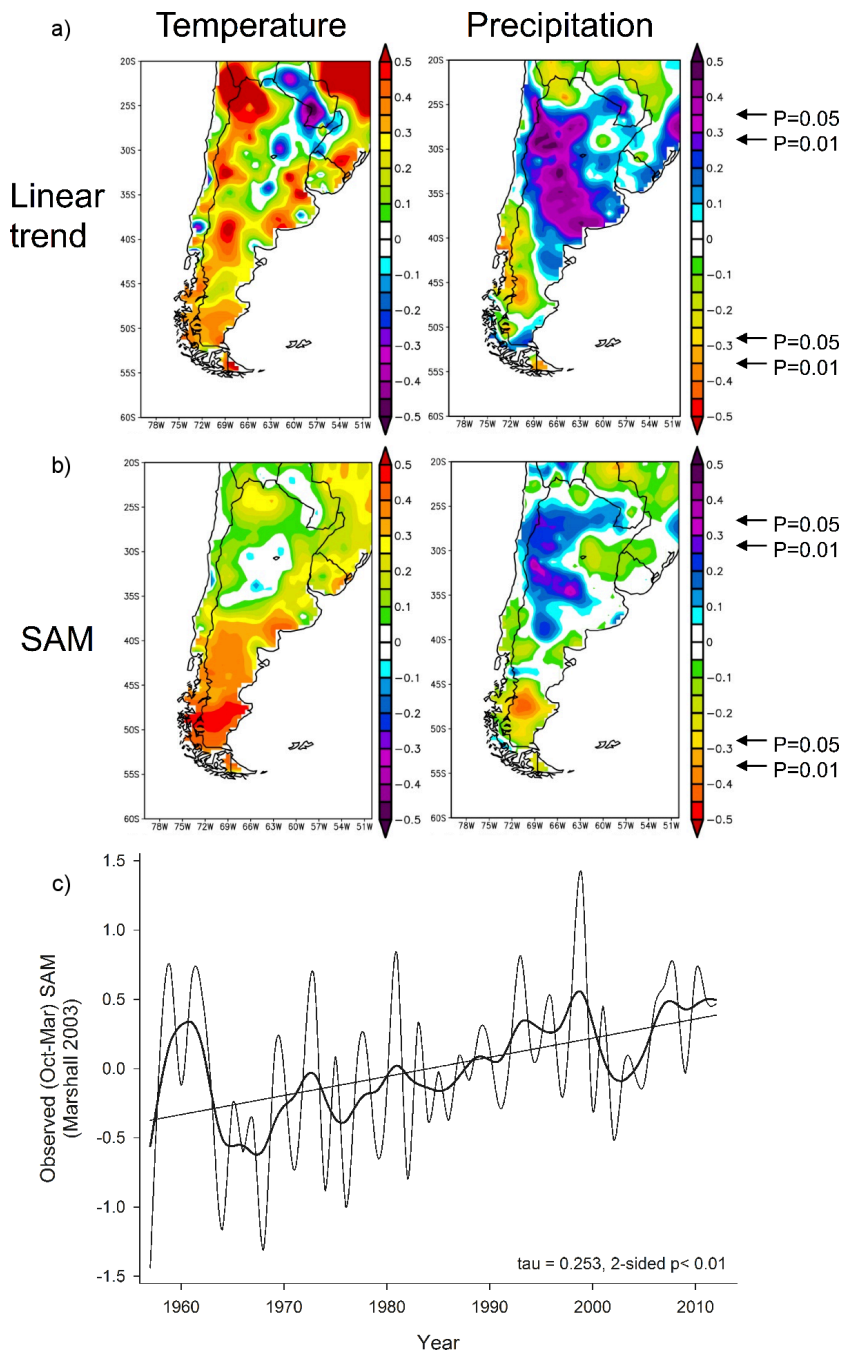
SAM has been shown to be a major driver of fire activity across the broad range of ecosystem types from semi-arid to rainforest ecosystems based on short (1984-2010) documentary fire records (3) and over a centennial time scale (ca. 1800-present) for particular forest types based on tree-ring fire histories (7, 18). However, we lack a comprehensive understanding of SAM's influence on fire activity over multiple centuries and at a broad latitudinal extent of forest ecosystems in SSA. We hypothesize that in biomass-rich temperate forests extending from c. 37° to 55° S in SSA, the SAM promotes fire primarily by enhancing warm spring-summer conditions that in turn desiccate fuels. Here we used 4,587 annually resolved fire-scar dates from 1,767 fire-scarred trees collected at 97 sites (the largest paleofire record yet assembled for the Southern Hemisphere) to reconstruct regional fire records for eight regions that extend from sub-tropical to sub-Antarctic latitudes in SSA and span the period from 990 to

Significance

Fire is a key ecological process affecting ecosystem dynamics and services, and is primarily driven by variation in fuel amount and condition, ignition patterns and climate. In the Southern Hemisphere, current warming conditions are linked to the upward trend in the Southern Annular Mode (SAM; due to ozone depletion). We use tree-ring fire scars obtained from subtropical dry woodlands through sub-Antarctic rainforests to assess the effect of SAM on regional fire activity over the past several centuries. Our findings reveal a tight coupling between fire activity and SAM at all temporal scales and in all biomes, with elevated wildfire synchrony and activity during the 20th century in comparison with previous centuries.

Reserved for Publication Footnotes

137
138
139
140
141
142
143
144
145
146
147
148
149
150
151
152
153
154
155
156
157
158
159
160
161
162
163
164
165
166
167
168
169
170
171
172
173
174
175
176
177
178
179
180
181
182
183
184
185
186
187
188
189
190
191
192
193
194
195
196
197
198
199
200
201
202
203
204



PDF

Fig. 1. Modern trend and teleconnections of climate with SAM in SSA. Spatial correlation between observed precipitation and temperature (Gridded [Jul-Feb] data; U Delaware) and a) a linear time series (i.e. 1, 2, 3...) for the 1949-2008 period, and b) observed (Jul-Feb) SAM (SAM) for the 1957-2008 period. c) Mean Spring-Summer (Oct-Mar) values of observed SAM for 1957-2012 (SAM (9, 12); <http://www.nercbas.ac.uk/icd/gjma/sam.html>). Significant correlation p-values at 0.05 and 0.01 are indicated with arrows in a) and b). In c) a linear fit and low-pass Gaussian filter (bold-line) is shown to highlight the low-frequency trend (11-yr window), and Kendall's tau statistic and 2-sided p-value are shown (the series also was tested for lag-1 correlation and proved not to be significant; $p > 0.05$).

205
206
207
208
209
210
211
212
213
214
215
216
217
218
219
220
221
222
223
224
225
226
227
228
229
230
231
232
233
234
235
236
237
238
239
240
241
242
243
244
245
246
247
248
249
250
251
252
253
254
255
256
257
258
259
260
261
262
263
264
265
266
267
268
269
270
271
272

2010 AD (Fig. 2a; *SI Appendix*, Table S1 and Fig. S1). From these fire-scar dates, indices of regional and sub-continental scale fire activity and synchrony were developed to examine relationships of the SAM and local and regional climate parameters across SSA at multiple time-scales. Our rationale is that at the regional and sub-continental scales high synchrony indicates a strong influence of climatic variations on fire (19) and overall high fire activity could reflect strong association with climate variability (19-21) as well as changes in ignition (i.e. either due to natural (22) or human (23-25) causes).

A recently developed proxy reconstruction of summer (Dec-Feb) SAM (9, 26) was used (Methods) to examine the relation of fire activity to variability in the SAM. This SAM reconstruction has proven useful in explaining tree growth variability in much of

our study area (26). We also tested for influences of variability of precipitation and temperature on fire activity at multiple scales, using proxy reconstructions of precipitation for southern South America (27) and of temperature for the Southern Hemisphere that is heavily weighted by the Pacific sector of the Southern Hemisphere, hence suitable for our study area (28) (hereafter, Precipitation index and Temperature index).

Results and Discussion

Reconstructed mean values of SAM during years of widespread fire (*no fire*) are significantly above (*significantly or trend below*) the long-term mean in all study regions located south of 37°S (*SI Appendix*, Figs. S2 and S3 and Text ST1). During the period of the instrumental records (1957-2013), higher (lower) values of SAM

273
274
275
276
277
278
279
280
281
282
283
284
285
286
287
288
289
290
291
292
293
294
295
296
297
298
299
300
301
302
303
304
305
306
307
308
309
310
311
312
313
314
315
316
317
318
319
320
321
322
323
324
325
326
327
328
329
330
331
332
333
334
335
336
337
338
339
340

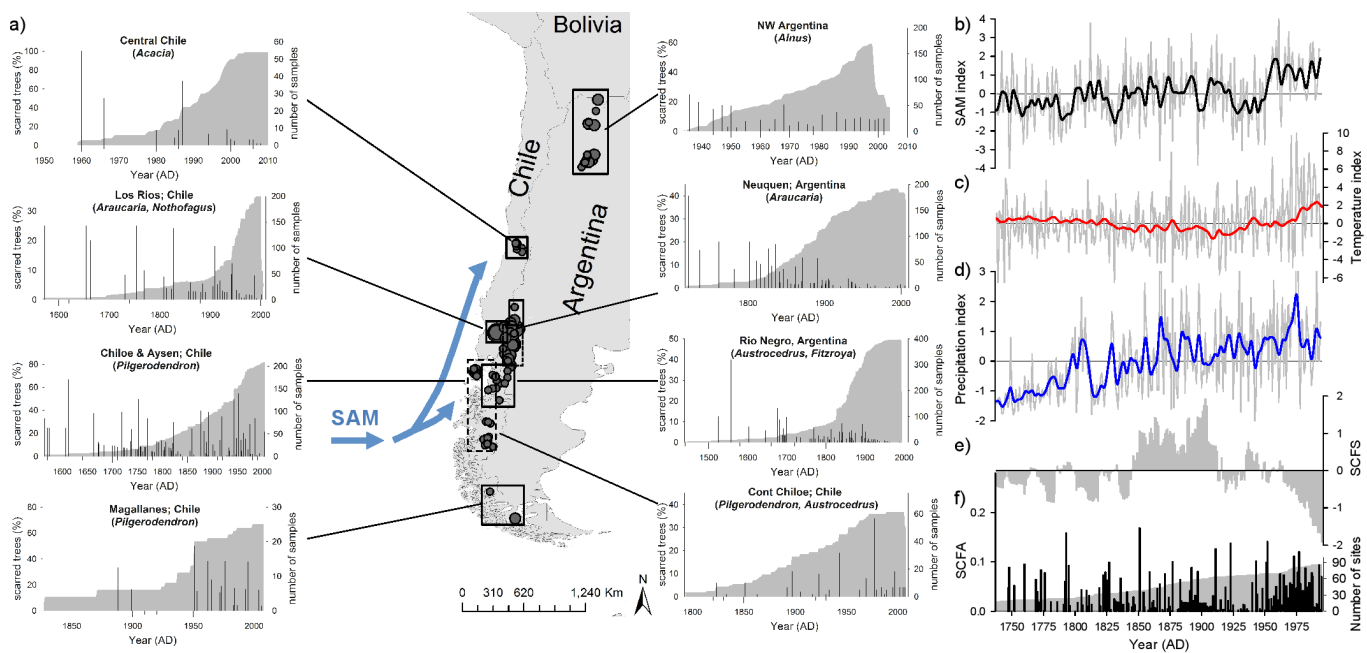


Fig. 2. Tree-ring based fire history and study regions (97 sites and 1767 fire scars) in southern South America (SSA). Study region locations (boxes on the map) and primary sampled species (in parenthesis) are indicated. Histograms show numbers of fire-scarred trees (%) and sample depth (grey area; starting when $\min \geq 3$ trees per region had been scarred at least once); note that x- and y-axes are not scaled equally in each region). Light-blue arrows indicate the geographical domain of the dominant extratropical forcing of regional climate variability, as represented by the Southern Annular Mode (SAM). Number of sites sampled within each region is depicted by the size of the black circles on the map. Graphs in the far right column show reconstruction of the SAM index departures (Dec-Feb; Marshall, black line; (26)), temperature departures (mean annual reconstruction for the Southern Hemisphere; red line; (28)), precipitation departures (total Dec-Feb southern South America reconstruction; blue line; (27)), Sub-Continental Fire Synchrony departures (SCFS; grey bars; 15-yr moving averages), Sub-Continental Fire Activity (SCFA; black bars) and total number of search sites (i.e. sample depth; grey fill). All climate series and the SCFS were standardized (z-scores) (in SD units), detrended and pre-whitened. All annually-resolved climate series (light grey lines) were smoothed with a 15-yr spline. Records from NW Argentina and Central Chile were not used for building the sub-continental fire indices due to their short sample depth.

Table 1. Correlation values (Pearson) of 15-yr smoothed time series (z-scores) of climate and fire§ (sub-continental fire activity, SCFA and synchrony, SCFS) over the 1738-1932 period (n =194).

Series	r values
SCFA vs. SAM	$r = 0.20^{***}$
SCFA vs. Temperature	$r = 0.12^*$
SCFA vs. Precipitation	$r = -0.09$
SCFS vs. SAM	$r = 0.18^{**}$
SCFS vs. Temperature	$r = -0.05$
SCFA vs. Precipitation	$r = 0.24^{***}$
SCFA vs. SCFS	$r = 0.07$

All reconstructions are filtered with a 15-year spline to emphasize the correlation among the low-frequency of all records. All time series were detrended. Pearson correlation coefficients in parentheses were calculated from pre-whitened series using the Trend Free Pre-whitening (TFPW) procedure in the zyp R package. §The sub-continental fire indices were built using a constant number fire recording sites over the 1738-1932 period. Significance p levels are: *0.05, **0.01, ***0.001.

are correlated with higher (lower) temperatures and reduced (increased) precipitation in most seasons of the year, including the fire season (*SI Appendix*, Fig. S4). In all study regions south of 37°S in SSA, the overall pattern is one of increased fire activity driven by fuel desiccation (rather than by insufficient quantity of fine fuel; *SI Appendix*, Text ST1) associated with positive SAM, which closely coincide with and is supported by results and interpretations from modern area burned-climate relationships in woody vegetation over the 1984-2010 period (3).

The collective fire history of all study regions' chronologies south of 37°S combined (minimum 2 trees and 10% of recorder trees per site) shows a rapid decline from early in the record (1400s AD) to the ca. 1700s, when fire activity increases gradually (1400s AD) to the ca. 1700s, when fire activity increases gradually (*SI Appendix*, Fig. S1). Starting in ca. 1850s fire activity increases very abruptly and large fire years occur every ca.15-20 years until the 1920-1940s period, when fire activity drops. Starting in the ca. 1960s fire activity ramps up again until the present (*SI Appendix*, Fig. S1). The temporal pattern of collective fire history of all regions is similar to the standardized synthesis of all charcoal records located south of 30°S along western South America (29). The post-1960s increases in fire are primarily driven by fire activity at mid and high latitudes on the west side of Andes (Fig. 2a), where wildfires on the eastern Andean slope show the effects

341
342
343
344
345
346
347
348
349
350
351
352
353
354
355
356
357
358
359
360
361
362
363
364
365
366
367
368
369
370
371
372
373
374
375
376
377
378
379
380
381
382
383
384
385
386
387
388
389
390
391
392
393
394
395
396
397
398
399
400
401
402
403
404
405
406
407
408

409
410
411
412
413
414
415
416
417
418
419
420
421
422
423
424
425
426
427
428
429
430
431
432
433
434
435
436
437
438
439
440
441
442
443
444
445
446
447
448
449
450
451
452
453
454
455
456
457
458
459
460
461
462
463
464
465
466
467
468
469
470
471
472
473
474
475
476

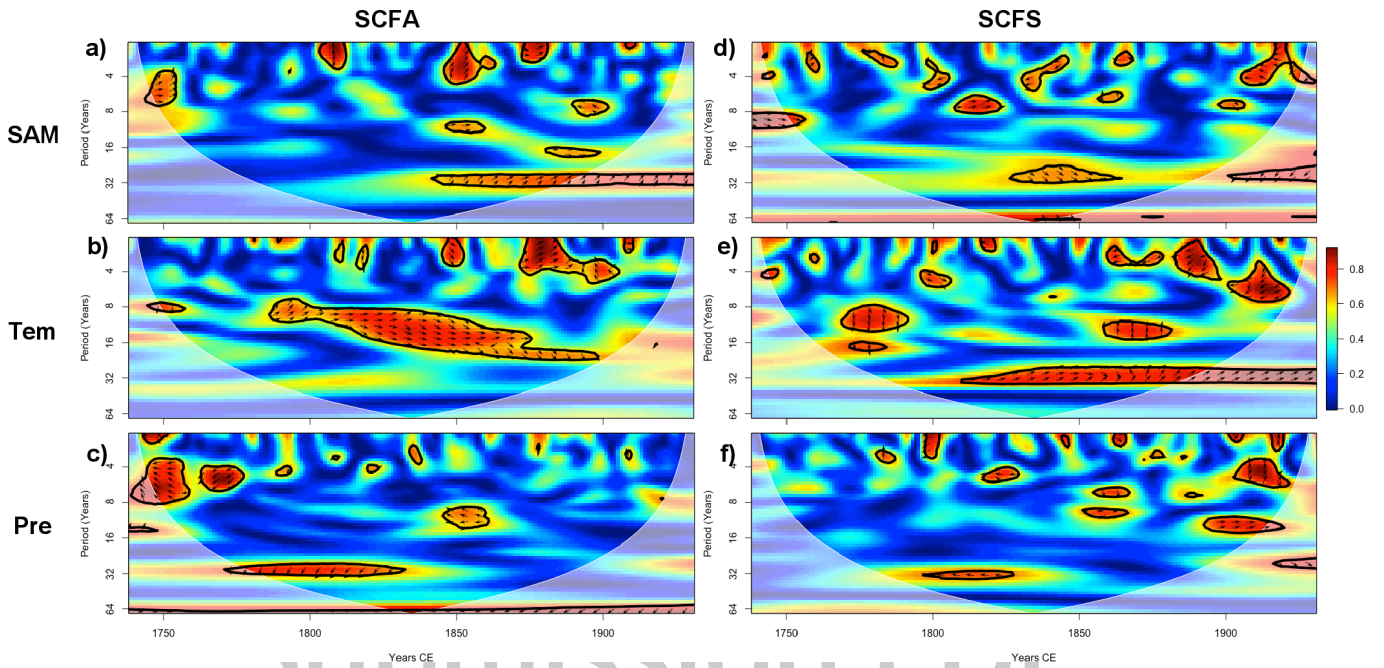


Fig. 3. Wavelet coherences between climate and fire at the sub-continental scale (Sub-Continental Fire Activity [SCFA; left column] and Sub-Continental Fire Synchrony [SCFS, right column]) and a) SAM, b) Temperature, and c) Precipitation reconstructions. Red regions in the plot indicate frequencies and times for which pairs of series are coherent. The cone of influence (white, dashed-line) and the significant coherent time-frequency regions ($p < 0.01$; 1000 Monte Carlo simulations; black solid line) are indicated. All figures were computed using standardized (i.e. z-scores) series that were detrended and pre-whitened (see Methods). Data sources: SAM (Dec-Feb; (9)), Temperature index (mean annual reconstruction for the Southern Hemisphere; (28)), and Precipitation index (total Dec-Feb southern South America reconstruction; (27)).

of active fire suppression since the 1930-40s (Fig. 2a). The sub-continental scale fire indices indicate that both the magnitude of fire activity (SCFA) and fire synchrony (SCFS) among regions have fluctuated over time and that in general there is not a clear relationship between these two indices (Fig. 2e,f). In contrast to the SCFA index, the amplitude in the SCFS index has increased over time with higher maximum and lower minimum values in the latter part of the analyzed period (1738-1932 AD) compared to early in the record.

Relatively weak but significant correlations were found for both sub-continental fire indices (SCFA [$r = 0.2$, $p < 0.01$] and SCFS [$r = 0.18$, $p < 0.01$]) and the SAM during the 1738–1932 period (Table 1). Series were pre-whitened to remove autocorrelation and the trend-free records were filtered with a 15-year spline to match the main spectra of the SCFA (Fig. S5). Likewise, similar low-frequency variability patterns are also shared between the Temperature and the SCFA indices ($r = 0.12$, $p < 0.01$) and between the Precipitation and the SCFS indices ($r = 0.24$, $p < 0.01$; Table 1).

The wavelet coherence patterns between the SCFA and both the SAM and the Temperature indices highlight numerous common short (ca. four 2-8 yr.) and longer (ca. two 10-18 yr.) periods throughout the record period with either in-phase and/or delayed in-phase coherence (Fig. 3a,b; *SI Appendix*, Text ST1). Similarly, the SCFS and SAM indices share similar numerous short (ca. three 4-8 yr.) and few longer (ca. 8-12-yr.) periods with either in-phase and/or delayed in-phase coherence (Fig. 3d). Some of the short period coherence might reflect the linkage of fire and the climatic parameters to ENSO variability documented in previous studies (5-7, 30, 31) but the goal of the current analysis was to identify the SAM signal in the coherence patterns. Only decadal-scale in-phase and/or delayed in-phase coherence (ca. 28-34-yr.) is shared between SCFS and temperature (Fig. 3e). Instead, precipitation and both fire indices share mostly anti-phase or delayed anti-phase coherence (i.e. drought and fire), with common numerous short (ca. 1-8 yr.) and fewer longer (ca. 8-10-yr.)

periods (Fig. 3c,f). Precipitation also shares a few common in-phase and/or delayed in-phase coherence of longer (ca. 10-16-yr.) periods with the SCFS (Fig. 3f). Overall, the wavelet coherence analyses on the SCFA also show a predominant role of drought in the first third of the record (i.e. ca. 1738 to 1825), whereas SAM and temperature increase in relevance over the remaining record (Fig. 3a-c). Similarly, an increase in the occurrence of coherences is also observed between the precipitation and the SCFS indices during the ca. 1780s-1930s period (Fig. 3f). Instead, no obvious change over time in coherences exists between the SCFS and both SAM and temperature indices (Fig. 3d,e).

The above results indicate that at the sub-continental scale, large wildfire years (SCFA) were primarily driven by warm conditions teleconnected with positive SAM during the 1738-1932 period. Some years of high synchrony in sub-continental fire activity are linked to reduced rainfall. In both cases our rationale in interpreting these results is that in SSA (and elsewhere (19, 20, 32) large fire years in cool and/or wet forests with abundant fuels and a short fire season have been commonly associated with periods of warm and dry conditions that reduce fuel moisture and favor fire activity. For the associations of high fire synchrony with above average precipitation, we speculate that those reflect spread of fires that initiated in fuel-limited grasslands adjacent to the core areas sampled for fire scars where previous research has shown a lagged association of fire and fine-fuel enhancing moister conditions (5, 33). This interpretation is consistent with the lagged association of fire with above-average moisture availability in grassland habitats throughout SSA based on modern climate-fire analyses using instrumental climate records and observations on annual area-burned (3).

Peaks in fire activity in the mid 1800s and early 1900s have been linked to coincident increases in human-set fires and climate variability in some of our study regions (6, 34, 35). While increases in fire frequencies in association with increased presence of indigenous and modern humans are detectable in particular habitats, periods of synchronous widespread fire documented at

477
478
479
480
481
482
483
484
485
486
487
488
489
490
491
492
493
494
495
496
497
498
499
500
501
502
503
504
505
506
507
508
509
510
511
512
513
514
515
516
517
518
519
520
521
522
523
524
525
526
527
528
529
530
531
532
533
534
535
536
537
538
539
540
541
542
543
544

545 annual resolution in tree-ring studies and at multi-decadal res- 619
546 olution in sedimentary charcoal studies have been more strongly 620
547 linked to climatic variability (4, 6, 34). Human amplification or 621
548 dampening of climate-induced trends in wildfire activity would 622
549 not have been synchronous across the six study areas given 623
550 different time periods for migrations of indigenous populations 624
551 and colonization by populations of European origin until the 625
552 1930s-1940s when fire records in some regions clearly reflect 626
553 fire exclusion (e.g. 7) while others reflect increased burning by 627
554 modern humans (34). Thus, we use the 1932 AD as a cut-off to 628
555 reduce the impact of modern changes in human ignition (Fig. 2a, 629
556 f; Methods) while acknowledging that in some regions pre-1932 630
557 human amplification and/or changes in lightning activity (1, 36) 631
558 may have affected both sub-continental scale indices (SCFA and 632
559 SCFS).

560 Conclusions and implications

561 In SSA wildfire activity is strongly associated with warm con- 633
562 ditions teleconnected with positive SAM at multiple time scales 634
563 both within large areas defined by particular forest ecosystem 635
564 types and at sub-continental scales across a broad range of forest 636
565 ecosystem types. At an interannual time-scale, widespread fires 637
566 across SSA co-occurred during anomalously high SAM conditions 638
567 over an extensive north-to-south gradient from ca. 37 to 54°S 639
568 based on 1252 scarred trees at 71 sites. Across this latitudinal 640
569 range, most study sites are dominated by forests ranging from 641
570 moderate to high-density stands in which fuel quantity is not 642
571 limiting to fire occurrence, and, instead, years of widespread fire 643
572 depend on fuel desiccation (*SI Appendix*, Text ST1). Ice core 644
573 and other proxies from Antarctica and southern South America 645
574 show that the positive trend in the SAM since the ca. 1940s is 646
575 at its highest level over at least the past thousand years (13), 647
576 and that atmospheric greenhouse gasses will keep forcing SAM 648
577 into its positive phase even if stratospheric ozone returns to 649
578 normal levels (12, 37). Atmospheric greenhouse gases are also 650
579 expected to force more frequent extreme El Niño events (38) 651
580 which previously have been shown to be strongly associated with 652
581 years of large wildfire activity in SSA (mainly north of 44°S) 653
582 both directly and in combination with positive SAM at the intra- 654
583 regional scale (*SI Appendix*, Tables S2 and S4). During the 2016- 655
584 17 fire season more than half a million hectares affected the 656
585 zone between ca. 29 to 40°S (ca. 3-5% of only that latitudinal 657
586 zone) were burned in central and southern Chile driven by a 658
587 long-lasting drought that was amplified by concurrent positive 659
588 SAM and ENSO conditions. While wildfire activity is expected to 660
589 continue to reflect interannual variability related to ENSO, the 661
590 continued dominance of the SAM as the primary driver of extra- 662
591 tropical climate variability in the Southern Hemisphere (11, 37) 663
592 portends increased wildfire activity in southern South America 664
593 for the 21st century. 665
594

595 Methods

596 *Study sites and species.* Tree ring fire-scar records were obtained from the 666
597 International Multiproxy Paleofire Database (IMPD), and from published 667
598 and unpublished sources (*SI Appendix*, Table S1). This dataset consists of 668
599 1767 fire-scarred trees from 97 sites in SSA extending from northwestern 669
600 Argentina to southern Patagonia, which were grouped into eight regions 670
601 of homogeneous climate variability (Fig. 2a) (following (3)). Ecosystems 671
602 included range from relatively dry woodlands and forests to mesic and rain 672
603 forests and bogs. 673

604 *Indices.* We created regional and sub-continental scale indices of years 674
605 of fire activity to highlight and test for changes at interannual and decadal- 675
606 scales. Following (24, 39), annual indices of fire occurrence (i.e. fire index) 676
607 were calculated for each of the 97 sites by dividing the number of fire-scarred 677
608 trees per year (with a minimum of two) by the number of trees potentially 678
609 recording fire in that year. The start and end dates of each site fire index 679
610 were determined by a minimum of four samples capable of recording fire. A 680
611 region-wide fire index (for each of our eight regions) was then calculated as 681
612 the sum of the site indices per year divided by the number of sites recording 682
613 fire in that year (*SI Appendix*, Table S3). A sub-continental scale fire activity 683
614 index (SCFA) was then calculated as the sum of the regional fire indices per 684
615 year divided by the number of regions recording fire in that year (Fig. 2f).

A sub-continental fire synchrony index (SCFS; modified from (19)), was 619
developed where annual fire synchrony between paired regions was identi- 620
fied by calculating over a centered 15-year period the number of fire years 621
recorded in both regions divided by the number of fire years recorded in 622
either region. This procedure was repeated in the 15 possible combinations 623
of pairs of the six regions (i.e. the two northernmost region's records were 624
too short and thus not included) and summed as total fire synchrony or SCFS 625
(Fig. 2e).

A cutoff date of 1738 AD was chosen for all statistical analyses (see 626
below) to ensure a minimum sample of recording sites ($n = 8$, $>10\%$), a 627
sufficient and commonly used percentage to characterize fire regimes in SSA 628
(6, 7, 18, 30, 31). In addition, the time period analyzed ends in 1932, when the 629
earliest known effective fire suppression in SSA is evident in the fire records 630
of the Río Negro and Neuquén regions and a pulse of fire activity is initiated 631
in the 1940s in the Aysén region associated with modern frontier activity and 632
road construction (Fig. 2a; *SI Appendix*, Tables S1 and S3).

The annually-resolved reconstructions of the SAM (Fig. 2b), the South- 633
ern Hemisphere mean annual temperature (hereafter Temperature index 634
(28); Fig. 2c), and the southern South America summer precipitation (Dec- 635
Feb; hereafter Precipitation index (27); Fig. 2d) were obtained from the 636
Paleoclimatology Datasets of NOAA's National Centers for Environmen- 637
tal Information[1]. The SAM reconstruction was developed from tree-ring 638
records; and the Temperature and Precipitation reconstructions were devel- 639
oped from tree-rings, marine and lake sediments, ice cores, documentary, 640
coral and speleothem records (*SI Appendix*, Text ST1). Although several SAM 641
reconstructions have been developed (13, 26) they all share some of the same 642
proxies (i.e. tree-ring chronologies) and consequently are not independent 643
reconstructions. We decided to use the SAM (i.e. based on the Marshall 644
index (9)) reconstruction because: a) the instrumental index used to build 645
the SAM reconstruction is based on sea-level atmospheric pressure records 646
from stations located between 40 and 65°S, rather than reanalysis data (SAM 647
NCEP-NCAR), which has been shown to magnify the strengthening of the 648
SAM signal over past decades (9), b) the region (40-65°S) used to build the 649
index is more relevant to our study area than locations of proxies used in 650
other reconstructions (13, 26), c) the summer season (i.e. Dec-Feb) of the SAM 651
reconstruction strongly correlated with summer weather in the study areas 652
which is the key variable affecting fuel desiccation (13), and d) analyses based 653
on an alternative SAM reconstruction (SAM-NCEP (26)) built from seasonal 654
(Dec-Feb) indices are very similar (not included). 655

Seasonal subsets of monthly gridded precipitation and temperature 656
(0.5x0.5 degrees; CRU TS3.22; 1901-2013) data used to conduct bootstrapped 657
correlation functions (see below) were derived for each study region as 658
defined by the boxes on the map in Fig. 2a. The instrumental index of the 659
SAM used was Marshall's summer (Dec-Feb) index (9), which is based on 660
selected station pressure records between 40 and 65°S over the period 1957- 661
2013. This instrumental SAM index is strongly correlated with tree growth in 662
SSA (26). 663

Statistical analyses. Three analyses were conducted to examine the 664
spatio-temporal relationships of wildfire activity in SSA to variability in the 665
SAM, precipitation and temperature reconstructions. First, at the regional- 666
scale we determined interannual-scale departures from long-term mean 667
SAM during years of widespread fire (and non-fire years) in each of the study 668
regions using Superposed Epoch Analysis (SEA) (33) in the dplR package (40) 669
in R (41) (*SI Appendix*, Fig. S2). For the SEA, years of widespread fire within 670
each study area were defined as years when ≥ 2 trees were scarred with a 671
minimum of four trees capable of recording fire per site at 10% or more sites 672
(i.e. region-wide fire index for each of our eight regions). A 5-year window 673
of mean SAM was centered on years of widespread (and no fire scar; Fig. 674
S3) fire for each of the study regions. Significance levels of the departures 675
from the long-term mean were determined from bootstrapped confidence 676
intervals (95%) estimated from 10,000 Monte Carlo simulations (42). Modern 677
teleconnections of the instrumental SAM index to local climate variability 678
(mechanistically responsible for variability in wildfire activity) were examined 679
with bootstrapped correlation functions (using the bootRes (43) package) 680
relating the observed SAM and seasonal gridded climate data for each of 681
the eight study regions (as defined by boxes on map in Fig. 2a; *SI Appendix*, 682
Fig. S4). The results of this first analysis were compared to those obtained 683
from modern relationship (significant [$p < 0.05$] correlation) between seasonal 684
observations of both climate parameters and SAM and annual area burned 685
in woody vegetation over the 1984-2008 period (results from (3); Table S4). 686

Secondly, at the sub-continental scale wavelet coherence was used to 687
test whether fire activity and climatic parameters who similar periodicities, 688
using the Biwavelet package in R. Wavelet coherence identifies regions in 689
time and space where two variables co-vary and is especially suitable for 690
the analyses of non-Gaussian time series, including climate and fire data 691
(32). The Morlet continuous wavelet transform was applied and the data 692
were padded with zeros at each end to reduce wraparound effects (44). We 693
only plotted phase arrows indicating direction of the correlation when the 694
wavelet coherence power was greater than the 90% percentile (Fig. 3). Al- 695

[1] <https://www.ncei.noaa.gov/>

681 though no difference in the coherence patterns were found when compared
682 to analyses conducted using standardized [z-scores] alone or standardized
683 and detrended time series, before conducting wavelet analyses, time series
684 were standardized (to z-scores) and trends and serial autocorrelation were
685 removed by using autocorrelation functions and autoregressive moving
686 average models (Trend-Free Pre-Whitened; using the Yue-Pilon method (45)
in the zyp package in R).

687 Thirdly, and also at the sub-continental scale, correlation functions
688 (Spearman) were used to test the long-term (decadal-scale) relationships
689 between the reconstructed SAM, the climate parameters, and both sub-
690 continental fire indices (SCFA and SCFS; Table 1). To highlight decadal-scale
691 variability in climate-fire relationships, we used Singular Spectral Analysis
692 to determine the dominant periods at which variance occurs in the SCFA index
693 (46); specifically, we used the Multi-Taper Method (MTM (47)) and identified
694 a window of 15 years, as one of the cycles that explain significant proportions
695 of variance in the SCFA over the 1738-1932 period (Fig. S5). We used the 15-yr
696 window to construct smoothed SCFA and the climate time series and to also
697 build the SCFS. To ensure that the correlation coefficients computed in this
698 third step were not influenced by changes over time in the sample depth (i.e.

1. Veblen TT, et al. (2011) Adapting to global environmental change in Patagonia: What role for disturbance ecology? *Austral Ecology*.
2. Johnston FH, et al. (2012) Estimated Global Mortality Attributable to Smoke from Landscape Fires *Environmental Health Perspectives* 120(5):695-701.
3. Holz A, Kitzberger T, Veblen TT, & Paritsis J (2012) Ecological and climatic controls of modern wildfire activity patterns across southwestern South America. *Ecosphere* 3(11):103.
4. Whitlock C, Moreno PI, & Bartlein P (2007) Climatic controls of Holocene fire patterns in southern South America. *Quaternary Research* 68(1):28-36.
5. Kitzberger T, Veblen TT, & Villalba R (1997) Climatic influences on fire regimes along a rain forest to xeric woodland gradient in northern Patagonia, Argentina. *Journal of Biogeography* 24(1):35-47.
6. Veblen TT, Kitzberger T, Villalba R, & Donnegan J (1999) Fire history in northern Patagonia: The roles of humans and climatic variation. *Ecological Monographs* 69(1):47-67.
7. Mundo IA, Kitzberger T, Roig Juñent FA, Villalba R, & Barrera MD (2013) Fire history in the Araucaria araucana forests of Argentina: human and climate influences. *International Journal of Wildland Fire* 22(2):194-206.
8. Thompson DWJ & Solomon S (2002) Interpretation of recent Southern Hemisphere climate change. *Science* 296(5569):895-899.
9. Marshall GJ (2003) Trends in the southern annular mode from observations and reanalyses. *Journal of Climate* 16(24):4134-4143.
10. Manatsa D, Morioka Y, Behera SK, Yamagata T, & Matarira CH (2013) Link between Antarctic ozone depletion and summer warming over southern Africa. *Nature Geosci* 6(11):934-939.
11. Gong D & Wang S (1999) Definition of Antarctic Oscillation Index. *Geophys. Res. Lett.* 26.
12. Thompson DWJ, et al. (2011) Signatures of the Antarctic ozone hole in Southern Hemisphere surface climate change. *Nature Geosci* 4(11):741-749.
13. Abram NJ, et al. (2014) Evolution of the Southern Annular Mode during the past millennium. *Nature Clim. Change* 4(7):564-569.
14. Garreaud RD, Vuille M, Compagnucci R, & Marengo J (2009) Present-day South American climate. *Palaeogeography Palaeoclimatology Palaeoecology* 281(3-4):180-195.
15. Sen Gupta A & England MH (2006) Coupled Ocean-Atmosphere-Ice Response to Variations in the Southern Annular Mode. *Journal of Climate* 19(18):4457-4486.
16. Garreaud RD (2007) Precipitation and Circulation Covariability in the Extratropics. *Journal of Climate* 20(18):4789-4797.
17. Silvestri GE & Vera CS (2003) Antarctic Oscillation signal on precipitation anomalies over southeastern South America. *Geophysical Research Letters* 30(21):2115.
18. Holz A & Veblen TT (2011) Variability in the Southern Annular Mode determines wildfire activity in Patagonia. *Geophysical Research Letters* 38:6 PP-6 PP.
19. Trouet V, Taylor AH, Wahl ER, Skinner CN, & Stephens SL (2010) Fire-climate interactions in the American West since 1400 CE. *Geophysical Research Letters* 37(4):L04702.
20. Kitzberger T, Brown PM, Heyerdahl EK, Swetnam TW, & Veblen TT (2007) Contingent Pacific-Atlantic Ocean influence on multicentury wildfire synchrony over western North America. *P.N.A.S. (U.S.A.)* 104(2):543-548.
21. Yao Q, et al. (2017) Pacific-Atlantic Ocean influence on wildfires in northeast China (1774 to 2010). *Geophysical Research Letters* 44(2):2016GL071821.
22. Abatzoglou JT, Kolden CA, Balch JK, & Bradley BA (2016) Controls on interannual variability in lightning-caused fire activity in the western US. *Environmental Research Letters* 11(4):045005.
23. Abatzoglou JT & Williams AP (2016) Impact of anthropogenic climate change on wildfire across western US forests. *Proceedings of the National Academy of Sciences* 113(42):11770-11775.
24. Taylor AH, Trouet V, Skinner CN, & Stephens S (2016) Socioecological transitions trigger fire

749 number of trees, sites and regions recording fire), we computed correlation
750 coefficients using a constant sample depth (10% of sites with fire-scarred
751 trees) over time over the 1738-1932 period (i.e. once the 10% criterion was
752 achieved new fire dates from recorder trees that started after 1738 were not
753 added into the regional chronologies).

Acknowledgements

754 This work was supported by the US National Science Foundation (AH,
755 TTV, JP; Awards 0956552 and 0966472), the Argentinian Council of Research
756 and Technology (JP, IM, TK; CONICET), Agencia Nacional de Promoción
757 Científica y Tecnológica of Argentina (JP; Awards PICT 2012-1891 and PICT
758 2012-0949), the Graduate School of the University of Colorado Boulder (AH,
759 JP), and the Center for Climate and Resilience Research (MEG; CONICYT/FON-
760 DAP/15110009). We thank Nerilie Abram, Eric Oliver, and Tarik C. Gouhier for
761 help with programing codes. **Author contributions** AH, TTV, and JP designed
762 the study. AH, TTV, IM, TK, HRG, MG, EA, JMQ, and CB contributed tree-ring
763 fire history data. AH and GW performed the analyses. AH, TTV, JP, IM, and TK
764 interpreted the results and wrote the paper. All authors discussed the results
765 and commented on the manuscript.

- regime shifts and modulate fire-climate interactions in the Sierra Nevada, USA, 1600-2015 CE. *Proceedings of the National Academy of Sciences* 113(48):13684-13689.
25. Marlon JR, et al. (2008) Climate and human influences on global biomass burning over the past two millennia. *Nature Geoscience* 1(10):697-702.
26. Villalba R, et al. (2012) Unusual southern Hemisphere tree growth patterns induced by changes in the Southern Annular Mode. *Nature Geoscience* 5:793-798.
27. Neukom R, et al. (2010) Multi-centennial summer and winter precipitation variability in southern South America. *Geophysical Research Letters* 37.
28. Neukom R, et al. (2014) Inter-hemispheric temperature variability over the past millennium. *Nature Clim. Change* 4(5):362-367.
29. Power MJ, et al. (2008) Changes in fire regimes since the Last Glacial Maximum: an assessment based on a global synthesis and analysis of charcoal data. *Climate Dynamics* 30(7-8):887-907.
30. Holz A & Veblen TT (2012) Wildfire activity in rainforests in western Patagonia linked to the Southern Annular Mode. *International Journal of Wildland Fire* 21(2):114-126.
31. González ME & Veblen TT (2006) Climatic influences on fire in Araucaria araucana-*Nothofagus* forests in the Andean cordillera of south-central Chile. *Ecoscience* 13(3):342-350.
32. Mariani M, Fletcher MS, Holz A, & Nyman P (2016) ENSO controls interannual fire activity in southeast Australia. *Geophysical Research Letters* 43(20):2016GL070572.
33. Baisan CH & Swetnam TW (1990) Fire history on a desert mountain range: Rincon Mountain Wilderness, Arizona, U.S.A. *Canadian Journal of Forest Research* 20:1559-1569.
34. Holz A & Veblen TT (2011) The amplifying effects of humans on fire regimes in temperate rainforests in western Patagonia. *Palaeogeography, Palaeoclimatology, Palaeoecology* 311(1-2):82-92.
35. Holz A, et al. (2016) Fires: the main human impact on past environments in Patagonia? . *PAGES Magazine* 2:72-73.
36. Garreaud RD, Gabriela Nicora M, Bürgesser RE, & Ávila EE (2014) Lightning in Western Patagonia. *Journal of Geophysical Research: Atmospheres* 119(8):4471-4485.
37. Gillett NP & Fyfe JC (2013) Annular mode changes in the CMIP5 simulations. *Geophysical Research Letters* 40(6):1189-1193.
38. Cai W, et al. (2015) ENSO and greenhouse warming. *Nature Clim. Change* 5(9):849-859.
39. Taylor AH, Trouet V, & Skinner CN (2008) Climatic influences on fire regimes in montane forests of the southern Cascades, California, USA. *International Journal of Wildland Fire* 17(1):60-71.
40. Bunn AG (2008) A dendrochronology program library in R (dplR). *Dendrochronologia* 26(2):115-124.
41. R Development Core Team (2016) A language and environment for statistical computing (Retrieved from <http://www.R-project.org>, Vienna, Austria).
42. Mooney CZ & Duval RD (1993) *Bootstrapping: A nonparametric approach to statistical inference* (Sage University Paper Series on Quantitative Applications to Social Sciences, Newbury Park, CA, U.S.A.).
43. Zang C & Biondi F (2013) Dendroclimatic calibration in R: The bootRes package for response and correlation function analysis. *Dendrochronologia* 31(1):68-74.
44. Torrence C & Webster PJ (1999) Interdecadal Changes in the ENSO-Monsoon System. *Journal of Climate* 12(8):2679-2690.
45. Yue S, Pilon P, Phinney B, & Cavadias G (2002) The influence of autocorrelation on the ability to detect trend in hydrological series. *Hydrological Processes* 16(9):1807-1829.
46. Vautard R & Ghil M (1989) Singular spectrum analysis in nonlinear dynamics, with applications to paleoclimatic time series. *Physica D: Nonlinear Phenomena* 35(3):395-424.
47. Mann ME & Lees JM (1996) Robust estimation of background noise and signal detection in climatic time series. *Climatic Change* 33(3):409-445.